# Integration of FEM-ANN Methods for Predicting the Horizontal Displacement of Barrette Walls

**Truong Xuan Dang**
Ho Chi Minh University of Natural Resources and Environment, Vietnam
dxtruong@hcmunre.edu.vn

**Luan Nhat Vo**
Faculty of Engineering and Technology, Van Hien University, Vietnam
luanvn@vhu.edu.vn

**Phuong Tuan Nguyen**
Mien Tay Construction University, Vinh Long Province, Vietnam
tuanphuongvk@gmail.com

**Hoa Van Vu Tran**
The SDCT Research Group, University of Transport Ho Chi Minh City, Ho Chi Minh City, Vietnam
hoa.tranvu.htgroup@gmail.com

**Tuan Anh Nguyen**
University of Transport, Ho Chi Minh City, Vietnam
tuanna@ut.edu.vn (corresponding author)

*Received: 26 December 2024 | Revised: 3 February 2025 | Accepted: 14 February 2025*

 *DOI: https://doi.org/10.48084/etasr.10026*

## ABSTRACT

**This study aims to evaluate and predict horizontal displacement ($U_X$, $U_Y$) and force (*Force*) of barrette walls during excavation through the integration of Finite Element Method (FEM) and Artificial Neural Networks (ANN). This approach is expected to optimize prediction accuracy, particularly under complex geological conditions. Initially, the FEM model was used to analyze the displacement and forces on the barrette walls in each excavation stage. The analysis results provided detailed data on displacement and forces, including position ($X$, $Y$, $Z$), axial forces ($N_1$, $N_2$), shear forces ($Q_{12}$, $Q_{23}$, $Q_{13}$), moments ($M_{11}$, $M_{22}$, $M_{12}$), and excavation depth (*Depth*). These data were then used as input to train the ANN model. With a structure comprising two hidden layers (64 neurons each) and one output layer (2 neurons), the ANN was evaluated using metrics such as MSE, RMSE, and $R^2$. The results showed that the ANN model achieved high prediction performance with an $R^2$ value of 0.9999, demonstrating its ability to accurately predict horizontal displacements. The importance analysis of the input features revealed that *Y*, *Depth*, and *X* were the most influential factors in the prediction results. The error between the predicted and actual values was minimal, highlighting the model's efficiency and reliability. Integration of FEM and ANN has proven to be an effective solution for analyzing and predicting the mechanical behavior of barrette walls. This method has great potential for broad application in the design and construction of geotechnical projects, especially in complex scenarios that require high accuracy.**

***Keywords-ANN; barrette wall displacement prediction; key feature evaluation; geotechnical modeling***

## I. INTRODUCTION

In large-scale construction projects, especially in areas with complex geological conditions, factors such as soil stratification, material heterogeneity, and fluctuating groundwater levels can significantly impact the mechanical behavior of retaining structures. Barrette walls play a crucial role in ensuring the structural stability of the project [1]. The primary function of barrette walls is to control deformation and bear the load from the surrounding soil, particularly during

deep excavation stages [2-4]. However, one of the greatest challenges is the occurrence of horizontal displacements and unexpected forces, which can directly affect structural stability and pose significant risks to adjacent structures. Precisely controlling these factors is a critical task in design and construction.

Traditional analytical methods, which predominantly rely on theoretical models or empirical formulas, often face limitations when applied to complex or nonlinear geological conditions [5-7]. This results in inaccuracies in predicting displacements and forces, thus reducing the effectiveness and safety of retaining wall systems [8-10]. In this context, the combination of the Finite Element Method (FEM) and Artificial Neural Networks (ANN) has emerged as a promising approach [11]. FEM is capable of simulating the mechanical behavior of the system in detail under real-world loading conditions, while ANN can learn from FEM data to provide more accurate predictions for various scenarios [12, 13]. This study aims to analyze the horizontal displacements and forces acting on barrette walls using the FEM method and develop an ANN model to predict the wall's behavior during the excavation phase. Combining these two methods not only enhances the accuracy of predictions but also offers a more efficient and flexible solution for the design and management of geotechnical projects. The results achieved are expected to contribute to improving the safety and efficiency of construction projects in the future.

## II. MATERIALS AND METHODS

The selected study area is characterized by two distinct soil layers. The upper layer consists of clay with a thickness of 7.5 m, while the lower layer comprises sand with a thickness of 32.5 m. These are common soil types in geotechnical engineering, each exhibiting unique mechanical properties that significantly influence the load-bearing capacity and deformation behavior of retaining wall systems. The Hardening Soil model is used in FEM simulations to accurately reflect the mechanical behavior of soil during deep excavation, particularly in terms of soil heterogeneity, groundwater influence, and non-linear behavior. The excavation area measures 11×44 m and is designed to reach a depth of 15.1 m. The site is adjacent to a one-story building, and the groundwater level is maintained at -4 m. These factors require the implementation of effective stability measures to minimize the risks associated with construction activities (Figure 1).

The structural system includes barrette walls, cap beams, and an H-beam shoring system designed to ensure stability and minimize wall deformation during excavation. The barrette walls are 800 mm thick and 25 m deep, capable of withstanding substantial loads under complex construction conditions. Above the barrette walls, an 800×800 mm cap beam is utilized to enhance horizontal stability, evenly distribute forces, and prevent horizontal wall displacements. Additionally, a multi-layer H-beam shoring system, with a cross-sectional dimension of 400×400 mm, is installed at depths of -1 m, -4.6 m, -7.1 m, and -9.6 m. This system plays a critical role in mitigating horizontal displacements ($U_X$, $U_Y$) and maintaining the stability of the retaining walls throughout the excavation process.

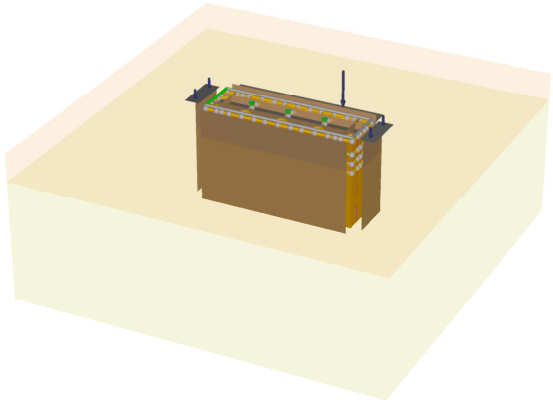

Fig. 1. 3D simulation of deep excavation pits.

The H-beam material used for shoring has a specific weight of 78.5 kN/m³, a cross-sectional area of 0.02187 m², and a modulus of elasticity of 210.0E6 kN/m², ensuring excellent load-bearing capacity under complex loading conditions. The cap beam, with a specific weight of 25 kN/m³ and a similar modulus of elasticity, significantly enhances the system's rigidity and horizontal load capacity. The barrette walls are designed with an elastic modulus of 32.5E6 kN/m² in two directions and a shear modulus of 16.25E6 kN/m², demonstrating excellent strength and deformation resistance.

The soil properties were analyzed and modeled using the Hardening Soil model. The clay layer has a saturated unit weight ($\gamma_{sat}$) of 20.57 kN/m², a deformation modulus ($E50_{ref}$) of 6875 kN/m², an internal friction angle ($\varphi'$) of 30.4°, and cohesion ($C'_{ref}$) of 7.1 kN/m². For the sand layer, $\gamma_{sat}$ is 20.55 kN/m², $E50_{ref}$ is 13.45E3 kN/m², and $\varphi'$ is 30°. Soil permeability was carefully defined, with horizontal permeability coefficients ($K_x = K_y$) of 3.59E-05 m/day for clay and 0.138E-3 m/day for sand, while vertical permeability coefficients were significantly lower. These parameters form the basis for building the FEM model and determining the mechanical behavior of the retaining wall system.

The research method integrates FEM analysis and ANN to predict horizontal displacements (Ux, Uy) and assess the impact of forces on barrette wall behavior during excavation. Initially, the FEM model was developed and implemented in Plaxis 3D using 10-node mesh elements to perform a detailed analysis of the mechanical behavior of the barrette wall system. The FEM model calculated displacements and forces at each excavation stage, corresponding to excavation depths of -2 m, -5.1 m, -7.6 m, -10.1 m, -13.1 m, and -15.1 m. The results included positions ($X$, $Y$, $Z$), forces ($N_1$, $N_2$), shear forces ($Q_{12}$, $Q_{23}$, $Q_{13}$), and moments ($M_{11}$, $M_{22}$, $M_{12}$), along with excavation depths, forming the input database for ANN development.

Subsequently, FEM data were used to train the ANN model [14]. The input data included 12 key features: positions ($X$, $Y$, $Z$), forces and moments ($N_1$, $N_2$, $Q_{12}$, $Q_{23}$, $Q_{13}$, $M_{11}$, $M_{22}$, $M_{12}$), and excavation depth (*Depth*). The output data comprised $U_X$ and $U_Y$, which are critical indicators of barrette wall displacement during excavation. The ANN model was trained on 285,264 FEM data points, ensuring representativeness and high accuracy, and was designed with two hidden layers, each

containing 64 neurons using the ReLU activation function and one output layer with two neurons. The model's performance was evaluated using metrics such as MSE, RMSE, MAE, $R^2$, and Adjusted $R^2$ [15]. Besides, the ANN model was validated using actual observed data during the excavation process, allowing for an assessment of its accuracy compared to real-world conditions.

## III. RESULTS

Finite Element Method (FEM) analysis has provided detailed insights into the horizontal displacement ($U_X$, $U_Y$) and forces and moments acting on barrette walls throughout the excavation process. The results indicate complex distributions of displacement and forces at different excavation stages, particularly in deeper layers where the walls are subjected to greater loads from soil pressure and groundwater.

Table I presents the statistical results of horizontal displacement $U_X$ and $U_Y$. The mean value of $U_X$ is -0.00396 mm, with a standard deviation of 0.361 mm, indicating minor deformation but considerable variation across different positions. Similarly, the mean value of $U_Y$ is -0.86 mm, with a standard deviation of 14.97 mm, reflecting uneven pressure impacts on the wall. At the sixth excavation stage, the maximum $U_X$ reached 2.92 mm, while the minimum was -2.98 mm, as shown in Figure 2. For $U_Y$, the displacement ranged from -0.05 mm to 0.05 mm (Figure 3). These findings show that maximum displacements tend to occur in deeper excavation layers.

In addition, forces and moments were analyzed in detail, as shown in Table II. The mean values of axial forces $N_1$ and $N_2$ are -353.12 kN/m and -93.55 kN/m, respectively, while shear forces $Q_{12}$, $Q_{23}$, and $Q_{13}$ exhibit significant variability, with standard deviations of 58.7 kN/m, 182.4 kN/m, and 171.2 kN/m, respectively. This reflects the complex impacts of soil pressure at different locations.

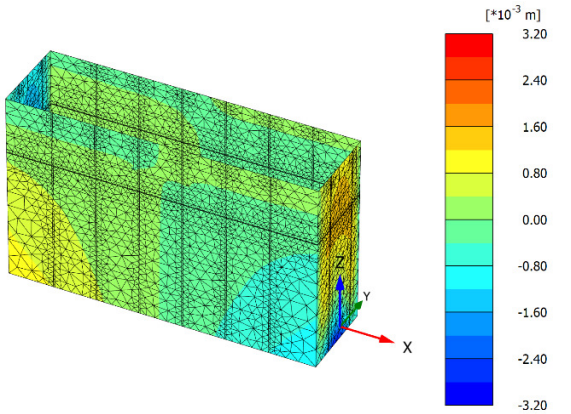


Fig. 2. Horizontal displacement ($U_X$) at the sixth excavation stage.

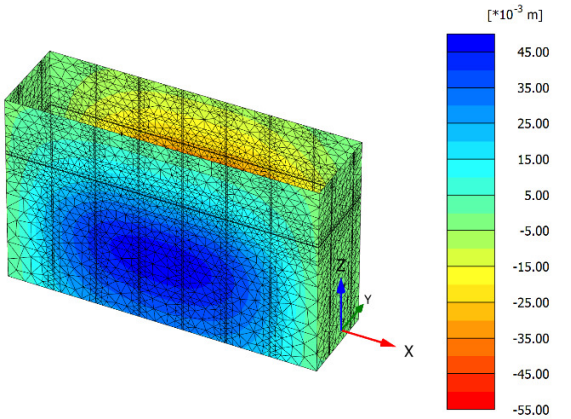


Fig. 3. Horizontal displacement ($U_Y$) at the sixth excavation stage.

TABLE I. STATISTICAL DESCRIPTION OF DISPLACEMENT RESULTS FROM FEM

| | Position (m) | | | Displacement (mm) | | | |
|---|---|---|---|---|---|---|---|
| **Var** | ***X*** | ***Y*** | ***Z*** | $U_X$ | $U_Y$ | $U_Z$ | ***U*** |
| **mean** | -0.00662 | 0.016905 | -10.9212 | -0.00396 | -0.86011 | 15.48028 | 19.90404 |
| **std** | 13.28192 | 5.064972 | 6.910253 | 0.361034 | 14.97476 | 6.346658 | 10.43367 |
| **min** | -20 | -5.5 | -25 | -2.988 | -50.888 | 3.904 | 3.907 |
| **25%** | -11.875 | -5.5 | -16.497 | -0.129 | -8.252 | 10.821 | 12.662 |
| **50%** | 0 | -0.278 | -9.277 | -0.004 | -0.46 | 17.133 | 20.133 |
| **75%** | 11.874 | 5.5 | -5.768 | 0.121 | 5.656 | 21.103 | 25.327 |
| **max** | 20 | 5.5 | 0 | 2.921 | 48.433 | 23.04 | 55.545 |

TABLE II. STATISTICAL DESCRIPTION OF FORCE RESULTS FROM FEM ANALYSIS

| **Var** | $N_1$ **(kN/m)** | $N_2$ **(kN/m)** | $Q_{12}$ **(kN/m)** | $Q_{23}$ **(kN/m)** | $Q_{13}$ **(kN/m)** | $M_{11}$ **(kNm/m)** | $M_{22}$ **(kNm/m)** | $M_{12}$ **(kNm/m)** |
|---|---|---|---|---|---|---|---|---|
| **count** | 285264 | 285264 | 285264 | 285264 | 285264 | 285264 | 285264 | 285264 |
| **mean** | -353.124 | -93.5506 | -0.16163 | -14.1166 | 0.25432 | 38.25936 | 70.20554 | -0.19033 |
| **std** | 320.2236 | 230.1036 | 58.70827 | 182.4501 | 171.2009 | 273.5645 | 242.0113 | 112.2483 |
| **min** | -2019.69 | -2752.27 | -1230.89 | -5251.2 | -2379.16 | -2349.47 | -1341.28 | -617.85 |
| **25%** | -563.138 | -207.108 | -10.1013 | -34.1948 | -36.004 | -11.274 | -26.036 | -24.1693 |
| **50%** | -309.599 | -48.4185 | 0 | 0 | 0.023 | 71.4145 | 2.861 | 0 |
| **75%** | -106.284 | 12.99425 | 9.54625 | 29.29525 | 36.25725 | 175.8393 | 107.65 | 23.91525 |
| **max** | 796.272 | 2809.171 | 1220.21 | 2364.668 | 2398.451 | 731.703 | 1389.799 | 617.38 |

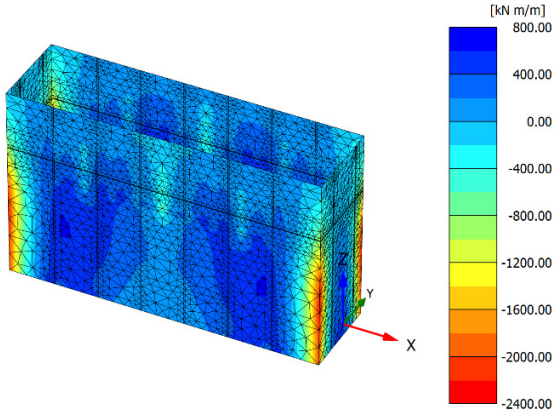


Fig. 4. Bending moment $M_{11}$ at the sixth excavation stage.

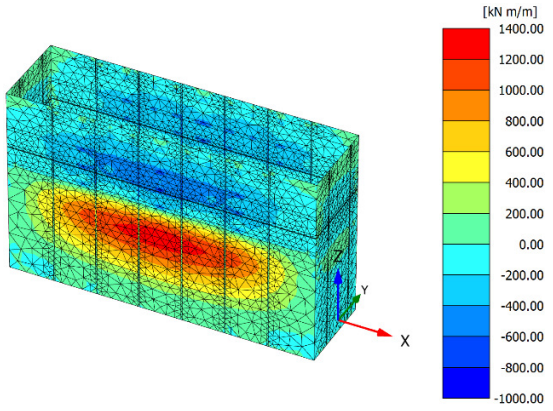


Fig. 5. Bending moment $M_{22}$ at the sixth excavation stage.

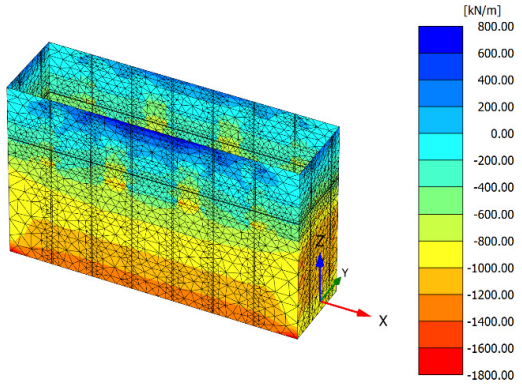


Fig. 6. Axial force $N_1$ at the sixth excavation stage.

Bending moments ($M_{11}$, $M_{22}$) and torsional moments ($M_{12}$) also show uneven distributions, with $M_{11}$ reaching a maximum of 654.5 kN m/m and a minimum of -2338 kN m/m (Figure 4), while $M_{22}$ ranges from -956.8 kN·m/m to 1389 kN·m/m (Figure 5).

Axial force $N_1$ varies between -1784 kN/m and 758.2 kN/m (Figure 6), while $N_2$ ranges from -2558 kN/m to 2809 kN/m (Figure 7). Notably, shear force $Q_{12}$ exhibits a large amplitude variation, from -893.6 kN/m to 897.1 kN/m (Figure 8), indicating uneven pressure distribution across the soil layers.

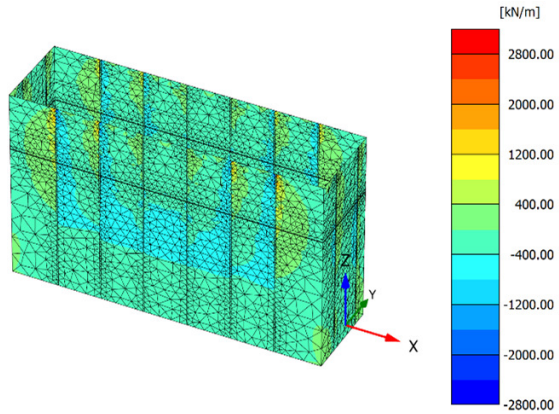


Fig. 7. Axial force $N_2$ at the sixth excavation stage.

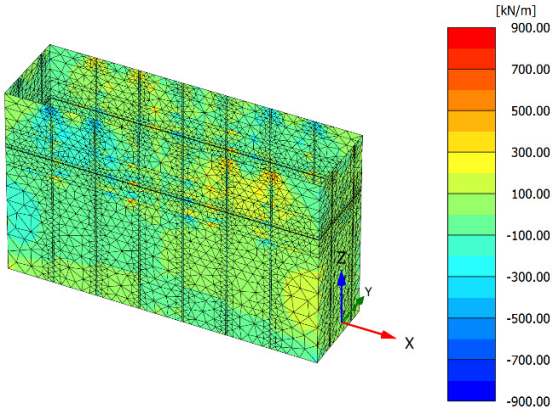


Fig. 8. Shear force $Q_{12}$ at the sixth excavation stage.

FEM analysis has provided reliable and detailed data for evaluating lateral displacements and loads on barrette walls throughout the excavation process. These results not only validate the accuracy of the finite element model but also serve as critical inputs for developing and training the ANN model used in this study.

The ANN model trained on FEM data demonstrated impressive predictive performance, as shown in Table III. The MSE value is 0.010959, and the coefficient of determination $R^2$ is as high as 0.999903, indicating that the model can explain nearly all variations in lateral displacements ($U_X$, $U_Y$) based on input features. These metrics affirm that the ANN is not only highly accurate but also well-suited for real-world data.

TABLE III. MODEL PERFORMANCE EVALUATION METRICS

| Metrics | Value |
|---|---|
| MSE | 0.010959 |
| RMSE | 0.104684 |
| MAE | 0.066327 |
| $R^2$ | 0.999903 |
| Adjusted $R^2$ | 0.999903 |

Figure 9 compares predicted values with test data (20% of the data from FEM analysis results), showing that the predicted data points almost overlap with actual values, with minimal deviation. The linear regression line between predicted and

actual values has a slope close to 1, further confirming the model's high accuracy. Minor errors between predictions and observations may result from negligible nonlinear factors in the data.

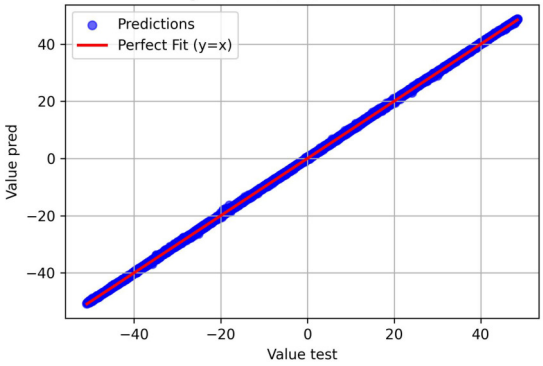


Fig. 9. Comparison of predicted values and test data.

Table IV presents an analysis of the importance of input features in influencing prediction outcomes. Variables *Y*, *Depth*, and *X* were identified as the most significant factors, with importance scores of 209.38, 52.19, and 35.35, respectively. This aligns with geotechnical theory, as factors such as horizontal position (*Y*), excavation depth (*Depth*), and coordinate (*X*) strongly affect the displacement of barrette walls. Other variables, such as moments ($M_{11}$, $M_{22}$, $M_{12}$) and forces ($N_1$, $N_2$), contributed less, as reflected in their lower importance scores.

TABLE IV. IMPORTANCE OF FEATURES INFLUENCING LATERAL DISPLACEMENT

| No. | Feature | Importance |
|---|---|---|
| 1 | *Y* | 209.3804 |
| 2 | *Depth* | 52.18696 |
| 3 | *X* | 35.34999 |
| 4 | *Z* | 29.82706 |
| 5 | $M_{11}$ | 1.118471 |
| 6 | $N_1$ | 0.377195 |
| 7 | $M_{22}$ | 0.01844 |
| 8 | $N_2$ | 0.017819 |
| 9 | $M_{12}$ | 0.00654 |
| 10 | $Q_{13}$ | 0.00167 |
| 11 | $Q_{12}$ | 0.001182 |
| 12 | $Q_{23}$ | 0.000313 |

The horizontal position (*Y*) significantly influences the displacement of the barrette wall due to the uneven distribution of the earth pressure along the horizontal axis. Excavation depth (*Depth*) plays a crucial role as soil stress increases with depth, leading to varying degrees of deformation at different excavation stages. Meanwhile, the longitudinal position (*X*) affects the wall displacement due to the influence of the support system and boundary conditions, altering the distribution of forces during construction.

The ANN model demonstrated outstanding ability in accurately predicting the lateral displacements of barrette walls while providing valuable insights into influential factors. The strong alignment between predicted values and empirical observations highlights the potential of ANN in supporting the design and management of geotechnical structures, particularly in complex scenarios such as deep excavation projects.

Table V shows a comparison between the predicted displacements from the ANN model and actual observational data measured by an inclinometer during the excavation process for different depths and positions. The discrepancies between the two values are minimal, with an average deviation not exceeding 1 mm, underscoring the high precision of the ANN model. These findings confirm that ANN can effectively predict and align with empirical data, making it a reliable tool for practical applications.

TABLE V. COMPARISON OF PREDICTED AND OBSERVED DISPLACEMENTS

| Position (m) | | | Depth (m) | Predicted (mm) | | Monitoring (mm) | | Difference (mm) | |
|---|---|---|---|---|---|---|---|---|---|
| *X* | *Y* | *Z* | | $U_X$ | $U_Y$ | $U_X$ | $U_Y$ | $U_X$ | $U_Y$ |
| 6.0 | 5.5 | 0 | -10.1 | 0.0 | -7.8 | 0.1 | -6.8 | -0.2 | -1.0 |
| 6.0 | 5.5 | 0 | -13.1 | 0.0 | -8.7 | -0.4 | -8.1 | 0.4 | -0.6 |
| 6.0 | 5.5 | 0 | -15.1 | 0.0 | -9.1 | 0.5 | -9.1 | -0.5 | 0.0 |
| 6.0 | 5.5 | 0 | -2 | 0.0 | -7.4 | 0.1 | -8.2 | -0.1 | 0.8 |
| 6.0 | 5.5 | 0 | -5.1 | 0.0 | -8.2 | 0.4 | -7.2 | -0.4 | -1.0 |
| 6.0 | 5.5 | 0 | -7.6 | 0.0 | -7.8 | -0.6 | -9.5 | 0.6 | 1.6 |
| 6.0 | -5.5 | 0 | -10.1 | 0.2 | 3.2 | 0.1 | 3.7 | 0.1 | -0.5 |
| 6.0 | -5.5 | 0 | -13.1 | 0.4 | 3.7 | 0.3 | 3.3 | 0.1 | 0.4 |
| 6.0 | -5.5 | 0 | -15.1 | 0.4 | 4.1 | 0.5 | 4.8 | -0.2 | -0.7 |
| 6.0 | -5.5 | 0 | -2 | 0.0 | 4.2 | 0.0 | 3.6 | 0.0 | 0.5 |
| 6.0 | -5.5 | 0 | -5.1 | 0.0 | 3.5 | 0.3 | 3.3 | -0.2 | 0.2 |

## IV. DISCUSSION

The FEM in this study was proven to be exceptionally effective in providing accurate data on lateral displacements ($U_X$, $U_Y$) and forces acting on barrette walls. The detailed insights from FEM not only form a reliable basis for analyzing the mechanical behavior of retaining wall systems but also directly support the development of the ANN model. Furthermore, FEM is highly dependent on initial assumptions about the physical parameters of the soil, leading to prediction errors if the input data are inaccurate. This approach contrasts with [6], where FEM was combined with ANOVA to identify factors influencing displacements and axial forces. Although both studies utilize FEM to analyze forces and displacements, the method in this study emphasizes the integration of FEM and ANN to enhance predictive capabilities.

The ANN model demonstrated superior performance in predicting lateral displacements, achieving a near-perfect $R^2$ value of 0.999903. This confirms the efficiency of ANN in learning and generalizing complex nonlinear data. Compared to [5], which used the Vlasov theoretical model to analyze lateral displacements of barrette walls in layered isotropic soils, the ANN model in this study offers wider applicability. It can accommodate experimental data from various conditions rather than relying solely on theoretical assumptions, as in the previous study.

The analysis of the importance of variables in the ANN model revealed that *Y* and *Depth* are the most significant factors affecting lateral displacements. This finding aligns well

with geotechnical theory, where horizontal coordinates and excavation depth play critical roles in the deformation of barrette walls. This study validated the model using actual observed data from the excavation process, showing that the error between predicted and measured values was minimal, confirming the practical applicability of the approach. The integration of FEM and ANN enhances the accuracy of horizontal displacement predictions, especially under complex geological conditions, compared to traditional methods based on empirical formulas or theoretical models, while also reducing computational time. However, this study is not without limitations. It focuses on a specific type of geological condition, meaning that the results need to be validated in other regions with more diverse conditions to enhance generalizability.

## V. CONCLUSIONS

This study demonstrated that the integration of FEM and ANNs is an effective solution for analyzing and predicting the mechanical behavior of barrette walls during excavation. FEM provides accurate and detailed data on displacements and forces, while ANN leverages this data to build a high-performance predictive model. The results of the ANN model, with an $R^2$ value of 0.9999, indicate exceptional accuracy compared to actual observational data. This underscores the strong applicability of the method in supporting the design and management of complex geotechnical projects. The FEM-ANN approach in this study can be scaled to large-scale geotechnical projects with multiple excavation stages due to its ability to learn from FEM data obtained from real-world projects with various soil types and construction conditions, allowing rapid predictions across different excavation scenarios. This research approach is not limited to the specific excavation site studied but has the potential for broader application to other excavation projects with similar structures. The ability to accurately predict lateral displacements and forces reduces construction risks, optimizes design, and improves the economic efficiency of construction projects. Future research directions could focus on expanding the model with real-world data from diverse locations and geological conditions to enhance the generalizability of the approach. In addition, integrating advanced technologies such as deep learning could further improve accuracy and the ability to handle complex datasets, enabling more reliable predictions for large-scale geotechnical construction projects.

## REFERENCES

[1] T. M. D. Do and T. Q. K. Lam, "Using Prestressed Reinforced Concrete Piles as Basement Walls for High-Rise Buildings," in *Sustainable Cities and Resilience*, Singapore, 2022, pp. 193–207, https://doi.org/10.1007/978-981-16-5543-2_16.

[2] C. Rabaiotti and C. Malecki, "In situ testing of barrette foundations for a high retaining wall in molasse rock," *Géotechnique*, vol. 68, no. 12, pp. 1056–1070, Dec. 2018, https://doi.org/10.1680/jgeot.17.P.144.

[3] H. Tan, Z. Jiao, F. Chen, and J. Chen, "Field Testing of Anchored Diaphragm Quay Wall Supported Using Barrette Piles," *Journal of Waterway, Port, Coastal, and Ocean Engineering*, vol. 144, no. 4, Jul. 2018, Art. no. 05018004, https://doi.org/10.1061/(ASCE)WW.1943-5460.0000456.

[4] T. X. Dang, P. T. Nguyen, T. A. Nguyen, and H. V. V. Tran, "Optimization of Barrette Wall Depths for Urban Excavation Stability Using FEM and ANOVA Testing," *Civil Engineering and Architecture*, vol. 12, no. 5, pp. 3530–3544, Sep. 2024, https://doi.org/10.13189/cea.2024.120529.

[5] Q. Wang, G. Cao, and L. Qu, "Lateral Behavior Analysis of a Rectangular Barrette in Layered Soil with Transverse Isotropy," *KSCE Journal of Civil Engineering*, vol. 28, no. 10, pp. 4329–4343, Oct. 2024, https://doi.org/10.1007/s12205-024-1915-5.

[6] L. N. Vo, T. X. Dang, P. T. Nguyen, H. V. V. Tran, and T. A. Nguyen, "A Novel Methodological Approach to assessing Deformation and Force in Barrette Walls using FEM and ANOVA," *Engineering, Technology & Applied Science Research*, vol. 14, no. 5, pp. 16395–16403, Oct. 2024, https://doi.org/10.48084/etasr.7975.

[7] A. B. Khan, S. W. Thakare, and A. I. Dhatrak, "Numerical Analysis of H-Shape Barrette Pile Subjected to Vertical and Lateral Loadings," in *Recent Developments in Geotechnics and Structural Engineering*, 2023, pp. 367–379, https://doi.org/10.1007/978-981-99-1886-7_31.

[8] H. Moayedi, M. Mosallanezhad, A. S. A. Rashid, W. A. W. Jusoh, and M. A. Muazu, "A systematic review and meta-analysis of artificial neural network application in geotechnical engineering: theory and applications," *Neural Computing and Applications*, vol. 32, no. 2, pp. 495–518, Jan. 2020, https://doi.org/10.1007/s00521-019-04109-9.

[9] C. E. Augarde, S. J. Lee, and D. Loukidis, "Numerical modelling of large deformation problems in geotechnical engineering: A state-of-the-art review," *Soils and Foundations*, vol. 61, no. 6, pp. 1718–1735, Dec. 2021, https://doi.org/10.1016/j.sandf.2021.08.007.

[10] G. Zheng, X. Yang, H. Zhou, Y. Du, J. Sun, and X. Yu, "A simplified prediction method for evaluating tunnel displacement induced by laterally adjacent excavations," *Computers and Geotechnics*, vol. 95, pp. 119–128, Mar. 2018, https://doi.org/10.1016/j.compgeo.2017.10.006.

[11] A. Baghbani, T. Choudhury, S. Costa, and J. Reiner, "Application of artificial intelligence in geotechnical engineering: A state-of-the-art review," *Earth-Science Reviews*, vol. 228, May 2022, Art. no. 103991, https://doi.org/10.1016/j.earscirev.2022.103991.

[12] M. Stoffel, F. Bamer, and B. Markert, "Artificial neural networks and intelligent finite elements in non-linear structural mechanics," *Thin-Walled Structures*, vol. 131, pp. 102–106, Oct. 2018, https://doi.org/10.1016/j.tws.2018.06.035.

[13] H. Liu, H. Su, L. Sun, and D. Dias-da-Costa, "State-of-the-art review on the use of AI-enhanced computational mechanics in geotechnical engineering," *Artificial Intelligence Review*, vol. 57, no. 8, Jul. 2024, Art. no. 196, https://doi.org/10.1007/s10462-024-10836-w.

[14] R. Acharyya, "Finite element investigation and ANN-based prediction of the bearing capacity of strip footings resting on sloping ground," *International Journal of Geo-Engineering*, vol. 10, no. 1, Mar. 2019, Art. no. 5, https://doi.org/10.1186/s40703-019-0100-z.

[15] T. Nguyen-Minh, T. Bui-Ngoc, J. Shiau, T. Nguyen, and T. Nguyen-Thoi, "Synergistic integration of isogeometric analysis and data-driven modeling for enhanced strip footing design on two-layered clays: Advancing geotechnical engineering practices," *Engineering Analysis with Boundary Elements*, vol. 167, Oct. 2024, Art. no. 105880, https://doi.org/10.1016/j.enganabound.2024.105880.